Analyst

Scattering and Absorption Differ Drastically in Their Inner Filter Effects on Fluorescence, Resonance Synchronous, and Polarized Resonance Synchronous Spectroscopic Measurements

Journal:	*Analyst*
Manuscript ID	AN-ART-04-2018-000790.R1
Article Type:	Paper
Date Submitted by the Author:	29-May-2018
Complete List of Authors:	Xu, Joanna; Mississippi state university, Chemistry Vithanage, Buddhini; Mississippi State University, Chemistry Athukorale, Sumudu; Mississippi State University, Chemistry Zhang, Dongmao; Mississippi State University, Chemistry

Analyst

ARTICLE

Scattering and Absorption Differ Drastically in Their Inner Filter Effects on Fluorescence, Resonance Synchronous, and Polarized Resonance Synchronous Spectroscopic Measurements

Received 00th January 20xx,
Accepted 00th January 20xx

DOI: 10.1039/x0xx00000x

www.rsc.org/

Joanna Xiuzhu Xu,[a] Buddhini C. Nugaduwa Vithanage,[a] Sumudu Athukorale,[a] and Dongmao Zhang *[a]

Sample inner filter effect (IFE) induces spectral distortion and affects the linearity between intensity and analyte concentration in fluorescence, Raman, surface enhanced Raman, and Rayleigh light scattering measurements. Existing spectrofluorometeric-based measurements treat the light scattering and absorption identically in their sample IFEs. Reported herein is the finding that photon scattering and absorption differ drastically in inducing the sample IFE in Stokes-shifted fluorescence (SSF) spectrum, resonance synchronous spectrum (RS2), and the polarized resonance synchronous spectrum (PRS2) measurements. Absorption with an absorption extinction as small as 0.05 imposes significant IFE on SSF, RS2, and PRS2 measurements. However, no significant IFE occurs even when the scattering extinction is as high as 0.9. For samples that both absorb and scatter light, one should decompose their UV-vis extinction spectra into absorption and scattering extinction component spectra before correcting the sample IFE. An iteration PRS2 method was introduced for the experimental decoupling the photon absorption and scattering contribution.The methodology presented in this work can be easily implemented by researchers with access to one conventional UV-vis spectrophotometer and one spectrofluorometers equipped with pair of excitation and detection polarizers. This work should be of broad significance in chemical research given the popularity of fluorescence spectroscopy in material characterization applications.

Introduction

Photon/matter interaction is undoubtedly one of the most fascinating phenomena in nature and have remained a central research topic in area of material characterizations, designs, and applications.[1-8] The most commonly used tools for studying the photon/matter interactions include UV-vis spectrophotometers and spectrofluorometers. UV-vis measurements provide information of collective contribution from the material photon absorption and scattering. Spectrofluorometer is a much more versatile instrument for probing material optical properties. With variable experimental settings, one can acquire the fluorescence excitation spectrum, Stokes-shifted fluorescence (SSF) spectrum,[9] resonance synchronous spectrum (RS2),[10] and recent polarized resonance synchronous spectra (PRS2).[11] RS2 and PRS2 signal of fluorescent samples can contain complex interplay of material photon absorption, scattering, fluorescence emission. Using combination of UV-vis and PRS2 measurements, one can decouple such interplay and experimentally quantify the material photon absorption, scattering, and emission activities.[7, 11, 12]One common problem for all spectrofluorometer-based measurements is however, the sample inner filter effect (IFE) that can induce spectral distortion and nonlinearity between intensity and sample concentration.[13-15] While it is known that the sample IFE occurs as long as there is photon absorption at the excitation and/or detection wavelengths in the SSF, RS2, and PRS2 measurements,[7, 16, 17] the role of sample light scattering has been obscure. In existing spectral data analyses, it is the sample total UV-vis extinction obtained directly from the UV-vis spectrophotometric measurements, rather than its absorption extinction component is used for the sample IFE correction.[18-20] The implicit assumption under this approach is that the light scattering induces the same degree of sample IFE as absorption. Another disturbing yet rather common literature practice is mislabeling sample UV-vis extinction spectra as its absorbance spectrum even for samples that contain light scatterers such as nanoscale to microscale particles.[21-24] As a side note one should always label the UV-vis spectrum as photon extinction, rather than absorbance. Photon extinction is a measurement of the light loss along its pass through the sampling cuvette, while absorbance describes the physical process responsible for such light loss.

Reliable correction of the sample IFE is critically important for reliable interpretation of the experimental data obtained in fluorescence study of fluorophore self-assembly,[24, 25] supramolecular formation,[26] and fluorophore interactions with nanoparticles.[27, 28] While these processes often lead to apparent fluorescence signal variations,[29] deducing the actual fluorescence

[a] Department of Chemistry, Mississippi State University, Mississippi State, Mississippi, 39762, United States

† Footnotes relating to the title and/or authors should appear here.
Electronic Supplementary Information (ESI) available: [details of any supplementary information available should be included here]. See DOI: 10.1039/x0xx00000x

activity for these samples can be challenging. This is because the higher-order structures formed through these processes are often simultaneous photon absorbers, scatterers, and fluorescence emitters. Separating the sample photon absorption and scattering contribution to their UV-vis extinction spectrum is not only a prerequisite for one to calculate the sample fluorescence quantum yield, but also for reliable fluorescence intensity quantification.

$$\frac{I^{corr}(\lambda_m)}{I^{obsd}(\lambda_m)} = 10^{0.5A(\lambda_x)+0.5A(\lambda_m)} \quad \text{Eq. 1}$$

$$\frac{I^{corr}(\lambda_m)}{I^{obsd}(\lambda_m)} = \frac{2.3\ d\ A(\lambda_x)}{1-10^{-d\ A(\lambda_x)}} 10^{g\ A(\lambda_x)} \frac{2.3\ s\ A(\lambda_m)}{1-10^{-s\ A(\lambda_m)}} \quad \text{Eq. 2}$$

Many sample IFE correction methods have been proposed for correcting the sample IFEs. The two example methods described by Eqs. 1 and 2 have been used extensively in literatures.[14, 30, 31] $A(\lambda_x)$ and $A(\lambda_m)$ are the UV-vis absorption extinction at the excitation and emission wavelengths, respectively. Eq. 1 is used for correcting the fluorescence IFE in spectra obtained with the standard 4 mL 1 cm × 1 cm cuvette. In this case the effective excitation and emission pathlengths are both assumed to be 0.5 cm. The correction parameters *d, s,* and *g* in Eq. 2 are instrument-specific parameters estimated on the instrumental configurations (excitation beam size, cuvette size, and others.[32] Substantial efforts have recently been devoted for achieving more reliable IFE corrections, including using derived absorption spectral profile[33], employing artificial neural networks[34], a nonlinear response model[35], multiple linear regression,[36] and parameter correction methods[37, 38].

$$\frac{I^{corr}(\lambda_m)}{I^{obsd}(\lambda_m)} = 10^{d_x\ A(\lambda_x)+d_m\ A(\lambda_m)} \quad \text{Eq. 3}$$

We have recently developed a sample IFE correction method that employed the correction equation of Eq. 3.[32] The d_x and d_m are the effective excitation and emission path lengths experimentally determined by the sample IFE on the solvent Raman signals induced by molecular chromophores. This solvent-Raman-based method is a performance-oriented approach, based on the criterion that the correct d_x, and d_m, in Eq. 3 should make IFE-corrected solvent Raman spectra perfectly overlapping regardless of the chromophore compositions.[32] These path lengths derived from the Raman measurements are instrument-specific, applicable to correcting the sample IFE on fluorescence spectra regardless of any excitation and emission wavelengths.[32]

All above methods were developed for correcting the sample IFE induced by photon absorption. In practice however, these equations have been used explicitly for correcting IFE induced by both light scattering and absorption extinction by replacing absorption extinction *A* in these equations with the sample total extinction intensity *E*, or implicitly when the material UV-vis extinction spectrum *E* is mislabelled as their absorbance spectra *A*.

Sample IFE can also affect the RS2 and PRS2 signal linearity as a functional of the sample concentration. Unlike the Stokes-shifted fluorescence (SSF) analysis in which the excitation and detection wavelength are different, the excitation and detection wavelength in both RS2 and PRS2 measurements are kept identical during the entire spectral acquisitions. The main difference between RS2 and PRS2 is that excitation and detection lights in RS2 are plane-polarized, but both are linearly polarized in PRS2 measurements. RS2 has been a popular method for studying fluorophore aggregations and fluorophore/nanoparticle interactions. Its signal was commonly assigned to the sample light scattering.[19, 20, 40-42] Indeed, several reports used RS2 method to determine the light scattering extinction spectrum.[19, 20] There are however several limitations with this approach. First, besides scattering, fluorescence can contribute to the RS2 spectra of the fluorophore-containing samples.[43] Second, RS2 is a fractional sampling technique, i.e, only a small portion of the scattered and/or fluorescence photons can be collected. The exact fraction of the collected photons depends not only on the instrument set-ups, but also on the fluorescence and light scattering depolarizations.[43] One should reliably resolve the undersampling problem in order to determine the material light scattering and fluorescence activities. In contrast, the PRS2 method provides a systematic approach to resolve these issues by experimentally quantifying the sample fluorescence and light scattering depolarization, and instrumental detector responses as a functional of the light polarizations and wavelengths.[43] Since both RS2 and PRS2 are acquired under resonance excitation and detection condition, photon absorption at this resonance wavelength imposes sample IFE on the signal intensity.[32] However, the sample IFE of light scattering on the RS2 and PRS2 signal has, to our knowledge, not been systematically examined.

Reported herein is a head-to-head comparison between the photon scattering and absorption extinctions in their sample IFE on SSF, RS2, and PRS2 measurements. One of the most critical finding is that the light scattering differs drastically from photon absorption in their IFEs. Over-correction occurs if one treats the light scattering the same as the sample photon absorption. Therefore, one should first decompose the sample UV-vis extinction spectrum into its absorption and scattering extinction component spectra before the sample IFE correction.

Experimental Section

Reagents and Equipment. The polystyrene nanoparticles (PSNPs, Cat # 16688) and the fluorescence polystyrene nanoparticles (*f*PSNPs, Cat # 18719), both with a nominal diameter of 0.1 μm were purchased from the Polysciences, Inc. All other chemicals were purchased from Sigma Aldrich and used as received. Fluorescent CdTe core-type quantum dots with the peak emission at 570 nm is abbreviated as QD (Lot#MKBV0066V). Molecular chromophores 2,4-dinitrophenyl hydrazine (DNPH) was used as a pure photon absorber. Nanopure water (18.2 *MΩ* cm, Thermo Scientific) was used in solution preparation. The UV-vis extinction spectra were acquired using a Thermo Scientific Evolution 300 UV-vis spectrophotometer. SSF, RS2, and PRS2 spectra were obtained with a Horiba Fluoromax-4-spectrofluorometer equipped with one computerized excitation and detection polarizers. All the spectra were acquired with a 1 cm × 1 cm 4 mL fluorescence cuvette.

UV-vis, Fluorescence, RS2, and PRS2 measurements. The UV-vis extinction spectra were acquired with a slit width of 2 nm. The spectral integration time was 0.3 s and slit widths of the both excitation and detection monochromator slit width were kept 2 nm

in all SSF, RS2, and PRS2 spectral acquisitions. The fluorescence emission, RS2, and PRS2 spectra are obtained by normalizing the signal from the sample detector with that from the reference detector (S1/R1). As such spectral variation due to wavelength- and/or time-dependent intensity variation in xenon lamp is eliminated. The SSF spectra of *f*PSNPs were acquired from 500 to 650 nm region with excitation wavelength of 400 nm. The QD SSF spectra were acquired with an excitation wavelength of 370 nm. All the PRS2 spectra shown in this work are solvent-background-subtracted before further data processing. The G-factor spectrum needed for correcting the instrument polarization bias in the light scattering and fluorescence depolarization measurements are obtained with the published procedure.[11]

Results and discussion

Sample IFE on the SSF measurements.

A head-to-head comparison of the sample IFE induced by light absorption and scattering was demonstrated with QD/DNPH (1st column, Fig. 1) and QD/PSNP mixtures (2nd column, Fig. 1). DNPH is a predominant light absorber with no significant light scattering, while PSNP is an approximately pure light scatterer with no significant light absorption. Therefore, the Fluorescence signal variations are due to absorption in QD/DNPH and scattering in QD/PSNP mixtures. In theory, PSNP and DNPH can induce QD fluorescence signal variation through a series of static and dynamic quenching, two near-field effects involving direct QD interactions with PSNP or DNPH, and the sample IFE, a far-field effect involving no direct QD interactions with PSNP or DNPH.[32, 44] In this work, the QD fluorescence signal variation induced by PSNP- and DNPH-addition should be due predominantly to the sample IFE induced by PSNP and DNPH, but not to dynamic and static quenching. This is because significant dynamic quenching occurs only when the quencher concentration is high (mM or above)[45, 46] and the mobilities of both the quencher and the fluorophore are relatively large.[44] Neither condition is applicable to the samples employed in this work. First, the DNPH and PSNP concentrations are very low. The highest DNPH and PSNP concentrations are 56.8 µM and 560 pM, respectively. Second, as a core-shell nanoparticle fluorophore with a nominal diameter around 6 nm (from vendor's specification), the mobility of the QD is likely significantly smaller than ordinary molecular fluorophores because of its large hydrodynamic radius, making the occurrence of dynamic quenching unlikely.

Static quenching involves formation of the ligand/emitter complex and such complex is fluorescent-inactive. The possibility of the significant static quenching can be ruled out by the control experiments that show UV-vis spectra of the QD/DNPH and QD/PSNP mixtures are equivalent to their summation spectrum of the respective component spectra (**Fig.S1, ESI**). This indicates that there is no QD/DNPH or QD/PSNP complex formation, or such complex formation has no significant impact on the QD optical properties.

The data in Fig.1 provides unequivocal evidence that light scattering and absorption differs substantially in their sample IFE. The total extinction in two sets of samples is increased from 0.1 to ~0.9 by the selected absorber DNPH (Fig. 1(A)) and scatterer PSNP (Fig. 1(B)), respectively. Evidently, the QD fluorescence reduction induced by DNPH (Fig. 1(C)) is drastically more significant than that by PSNP (Fig. 1(D)). The fluorescence intensity monotonically decreases with increasing DNPH concentration (Fig. 1(C)). Increasing collective photon absorption at excitation (370 nm) and

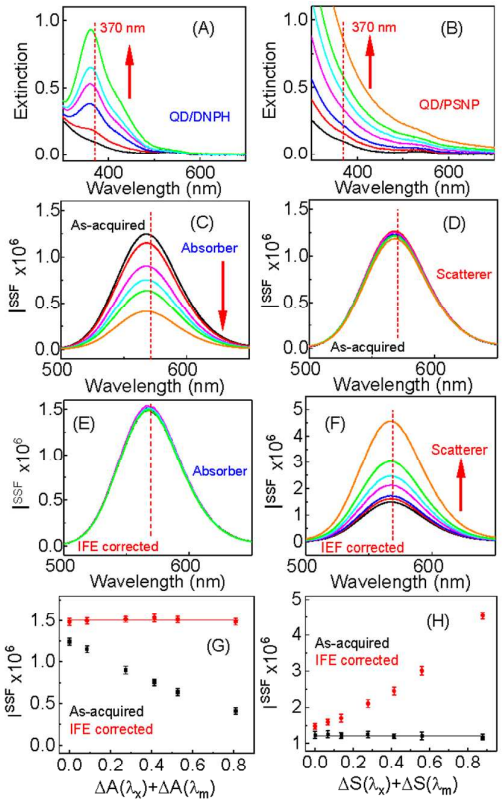

Fig.1 (A) and (B) are the UV-vis extinction spectra of QD spiked with DNPH and PSNP, respectively. (C) and (D) are the fluorescence spectra of QD/DNPH and QD/PSNP mixtures, respectively. (E) and (F) are sample-IFE-corrected spectra corrected with the effective pathlengths obtained based on the sample IFE on the solvent Raman signal. (G) and (H) are the QD fluorescence intensity as a function of the sample extinction increased by the DNPH photon absorption and PSNP scattering, respectively.

emission (570 nm) wavelength by 0.79 induces about 67% of QD fluorescence signal reduction. In contrast, there is no significant fluorescence signal attenuation in any of the PSNP-added samples, even when the collective light scattering extinction at the excitation and detection wavelengths as large as 0.90.

Using the effective path lengths (d_x=*0.46, and* d_m=*0.55*) and Eq. 3 determined with our recent work,[32] sample IFE induced by the photon absorption induced by DNPH were nearly perfectly corrected (Fig. 1E and 1G). However, overcorrection occurs when the same correction method is applied for the sample IFE induced by PSNP light scattering (Fig. 1(F) and 1(H)). Indeed, if one corrects the sample IFE induced by light scattering using the method developed for photon absorption, one would mistakenly conclude that the PSNP enhances QD fluorescence.

The data shown above is to our knowledge the first experimental demonstration that light scattering and absorption differs in their sample IFEs on SSF. While the sample IFE by photon absorption can be readily understood on the fact that light absorption permanently eliminates excitation and emission photons, the effect of the photon scattering on fluorescence signal

is much more complicated. Scattering only changes the trajectories of the scattered excitation and fluorescence photons, but doesn't eliminate the possibility for the scattered excitation photons to generate fluorescence photons or the scattered fluorescence signal to reach the detector. Quantitatively understanding the effects of such trajectory change and its impact on the fluorophore fluorescence signal is currently impossible. Conceptually, these effects depend not only on the sample light scattering intensity and fluorescence activity, but also on the light scattering and fluorescence depolarizations as well as the instrument response bias on the polarization of the emitted photons. As an example, scattering can change the excitation and fluorescence photon polarizations, thereby the number of the photons that can reach the detector. Nonetheless, the data obtained with PSNP/QD mixture indicates that empirically the sample IFE by light scattering is totally negligible even for the samples with photon scattering extinction as high as 0.75 at the excitation wavelength and the collective scattering extinction at the excitation and emission wavelengths as high as 0.90 (Fig. 1).

Sample IFE on RS2 and PRS2 measurements.

RS2 measurement involves only one spectral acquisition where both excitation and detection photons are polarized in the plane perpendicular to the propagation direction of the excitation or detection photons. In contrast, the PRS2 measurement involves two spectral acquisitions with excitation and detection polarization combinations of "VV" and "VH", respectively.[11] "V" refers to the light polarized linearly in the direction perpendicular to the plane defined by the light source, sample chamber, and detector, while "H" represents light linearly polarized parallel to this plane. The first letter in "VV" and "VH" refers to the excitation polarization, and second to the detection polarization.

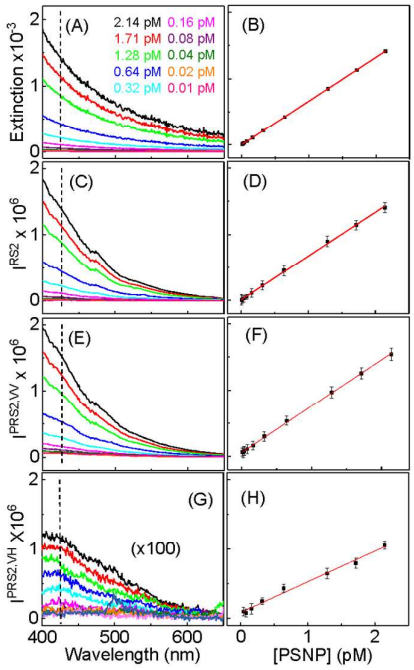

Fig. 2. (Left column) (A) UV-vis extinction spectra for a series of PSNP solutions with the specified concentrations. (C) RS2, (E) PRS2 VV, and (G) PRS2 VH spectra of the samples used in plot (A). (Right column) (B) PSNP UV-vis intensity as a function of PSNP concentrations for the wavelength highlighted in plot (A). (D), (F), and (H) are the RS2, PRS2 VV, and PRS2 VH intensity in plots (C), (E), and (G), respectively, as a function of PSNP concentrations. The black dots are as-acquired spectral intensities. The solid line is a linear-fitting of the black dots as a function of PSNP concentration. The dash lines in the left column figures indicate the spectral wavelength for the plots in the right

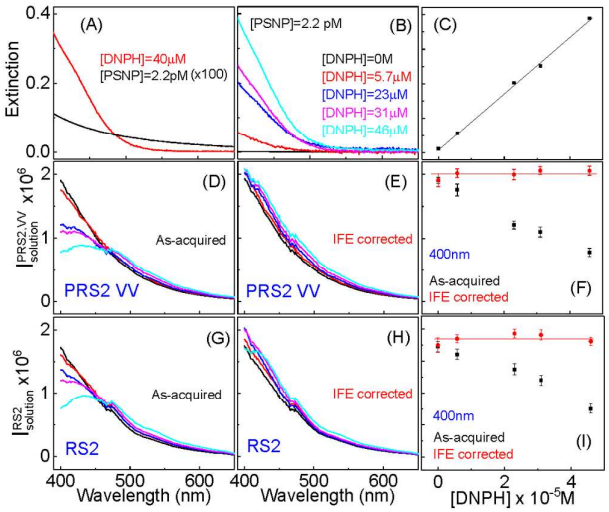

Fig. 3. (A) UV-vis extinction spectra obtained with 2.2 pM PSNP and 40 μM DNPH alone. (B) UV-vis extinction spectrum of PSNP/DNPH mixtures where the concentration of PSNP was kept constant (2.2 pM), but the DNPH concentrations vary as specified in the legends. (C) UV-vis extinction intensity at 400 nm as a function of the DNPH concentration. (D) as-acquired PRS2 VV spectra of the mixtures, (E) the sample-IFE corrected PRS2 VV spectra. (F) as-acquired and sample-IFE corrected PRS2 VV spectral intensity at 400 nm as a function of DNPH concentration. (G) as-acquired RS2 spectra, (H) the sample-IFE corrected RS2 spectra. (I) as-acquired and sample-IFE corrected RS2 spectral intensity at 400 nm as a function of DNPH concentration. The black dots in plots (C), (F), and (I) are as-acquired spectral intensities, and the red dots in plots (F) and (I) are the sample-IFE corrected intensities.

Light scattering and absorption also differ drastically in their IFE effects in the RS2, PRS2 VV, and PRS2 VH measurements. This is observed with the experimental data obtained with solutions containing PSNP alone (Fig. 2) and those of PSNP/DNPH mixture (Fig. 3). The PSNP-alone solutions can be treated as the scatterer-alone samples, while the PSNP/DNPH are mixtures of scatters and absorbers. Evidently there is no detectable sample IFE in the scatterer-only samples in the entire RS2 and PRS2 spectral region even when their signal reaches the instrument saturation intensity (Fig. 2(C) and 2(E)), which is 2,000,000 counts for the Fluoromax-4 used in this work. The RS2, PRS2 VV, and PRS2 VH spectra have an excellent linearity as a function of the PSNP concentration (Fig. 2(D), 2(F), and 2(H)), excluding the possibility of significant sample IFE in those samples. The reason that the PSNP PRS2 VH spectra

signal (Fig. 2(G)) is drastically lower than their PRS2 VV counterparts (Fig. 2(E)) is that the PSNPs have very small light scattering depolarization.[11]

The data in Fig. 2 indicates that for light scatterer-only sample, the light scattering should not be of a concern for any viable RS2, PRS2 VV spectral acquisitions in which the spectral intensities are below the instrument saturation intensity. This is because spectrofluorometer is extraordinarily sensitive to light scattering but with a finite dynamic range. Taking the Fluoromax-4 spectrofluorometer as an example, its PRS2 VV linear dynamic range in terms of scattering extinction at the 400 nm wavelength is from ~5.0×10^{-6} to ~2×10^{-3} for scatterer-only samples (**ESI**). This high sensitivity explains why spectrofluorometer can quantify the light scattering cross-sections even for small solvent molecules that are totally impossible with conventional UV-vis spectrophotometric measurements.[12] On the other hand, the finite linear dynamic range of the instrument detector explains why light scattering extinction is unlikely to induce significant sample IFE in practical RS2 and PRS2 measurements, at least for the ones conducted with the Fluoromax-4 spectrofluorometer. This is because the light scattering will saturate the detector response far faster than it becomes large enough to induce detectable sample IFE. The PSNP data shows that light scattering extinction as small as 0.002 is more than sufficient (Fig.s 2(A) and 2(B)) to cause the RS2 and PRS2 signal saturation (Fig.s 2(C) and 2(E)), while the data shown in Fig. 1 indicates that light scattering excitation as large as 0.90 remains insufficient to induce significant sample IFE.

According to Eq.3, the presence of photon absorbers shifts both the upper and lower linear dynamic limit of PRS2 and RS2 for light scattering samples by approximately a factor of $10^{A(\lambda,)d}$ where d is the sum of d_m and d_x, as photon absorption attenuates RS2 and PRS2 signal the same way as it does for SSF signal.[11] This result indicates that even for PRS2 and RS2 samples with photon absorption extinction as high as 1, their light scattering extinction remains negligibly small for imposing significant IFE. As an example, the presence of the light absorber at 400 nm with absorption extinction of 1 shifts the upper scattering extinction detection limit of the Fluoromax-4 instrument to 0.02, which is still insignificant for inducing detectable sample IFE.

One important implication of ultra-high RS2 and PRS2 sensitivity to light scattering is that one can directly use the sample photon extinction for the sample IFE correction for RS2 and PRS2 samples as long as the photon extinction is relatively small (<1, for example) and no signal saturation occurs in the as-acquired RS2 and PRS2 spectra. In this case, the light scattering extinction should be negligibly small, thus including it in the sample IFE correction should not induce significant overcorrection. Experimental demonstration of the effectiveness of this strategy is shown with the data obtained with the PSNP/DNPH mixtures (Fig. 3) where the concentration of PSNP is constant (2.2 pM), but the concentration of DNPH varies. Fig. 3(A) are the UV-vis spectra of the 2.2 pM PSNP sample and a DNPH control. The near perfect linearity between extinction intensity of PSNP/DNPH mixtures as a function of the DNPH concentration (Fig. 3(B) and 3(C)) suggests that either PSNP and DNPH has no significant direct interactions, or such interaction has no significant impact on the optical properties of either PSNP or DNPH. As a result, the PSNP PRS2 and RS2 signal attenuation induced by the DNPH addition can be assigned to the sample IFE imposed by the DNPH photon absorption.

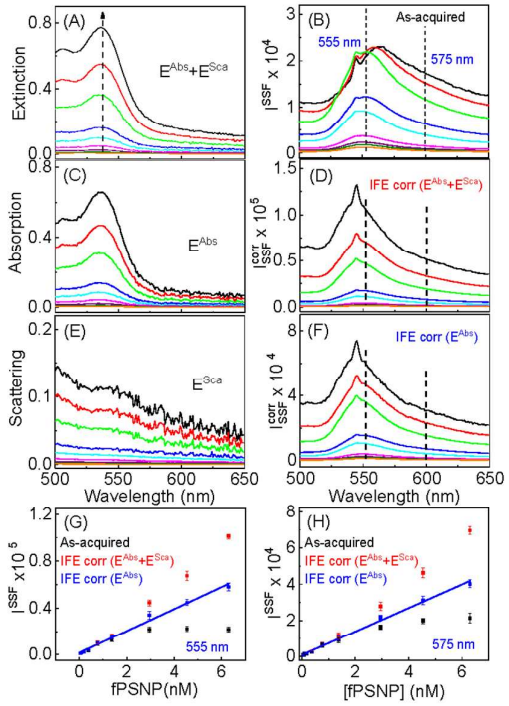

Fig.4 Experimental data obtained with the *f*PSNP. (A) UV-vis extinction spectra of the *f*PSNP with increasing concentrations indicated with the arrow, (B) as-acquired *f*PSNP fluorescence spectra, (C) and (E) the *f*PSNP absorption and scattering extinction spectra, respectively, obtained by iteration PRS2 decomposition of the UV-vis extinction spectra in (A). (D) IFE-corrected fluorescence spectra that uses the photon extinction for the IFE correction. (F) IFE-corrected fluorescence spectra that uses only the sample photon absorption extinction for the IFE correction. (G) and (H) the as-acquired and the sample-IFE corrected fluorescence spectral intensity as a function of *f*PSNP concentrations at the two representative emission

Apparently, the presence of DNPH induced significant sample IFE on the PSNP PRS2 and the RS2 signal (Fig. 3(D) and 3(G)). This IFE can be reliably corrected using Eq. 3 where the absorption extinction *A* is replaced by total photon extinction *E*. This confirms that one can use photon extinction directly for correcting the sample IFE in PRS2 and RS2 spectra obtained with Fluoromax-4 instruments or other spectrofluorometers with similar detector responses.

It is emphasized again that the reason this approach (using the total extinction directly for correcting the sample IFE) works well for the PRS2 and RS2 measurements conducted in this work is that the light scattering contribution is negligibly small to be either included or left out for the sample IFE correction. Indeed, the maximum light scattering extinction for the samples shown in Fig. 3 is ~0.002 (Fig. 3(A)). However, for RS2 and PRS2 measurements conducted less sensitive spectrofluorometers or highly upper limit of linear dynamic range, the sample saturation scattering extinction can be significantly higher. In this case, the effect of light scattering on the RS2 and PRS2 signal cannot be ignored. Therefore, it is necessary to

devise an analytical method capable of separating light scattering and absorption in PRS2 samples in which the light scattering can be significant.

Decomposition of sample UV-vis extinction spectrum with iteration PRS2.

Experimentally decomposing sample UV-vis extinction spectrum into its absorption and scattering extinction component spectra requires combined UV-vis and PRS2 measurements.[11] Prior to the PRS2 data analysis, however, one must reliably correct the sample IFE induced by sample photon absorption.[7, 11] This presents a dilemma that one needs to know the light scattering and absorption extinction in order to conduct the experimental decomposition of the sample UV-vis extinction spectrum into its scattering and absorption extinction component spectra. Fortunately, this dilemma can be readily resolved using an iteration PRS2 workflow described below.

Step 1: use the sample UV-vis intensity obtained with the UV-vis spectra to perform the sample IFE correction in the PRS2 measurement. The procedure of the IFE correction is described in recent reports. [7, 11] In this case, the total sample extinction is assumed to be the absorption extinction, i.e, an overestimated light absorption extinction (A^{OE}). This leads to overcorrection of the sample IFE in the experimental PRS2 spectra, and consequently an overestimated light scattering extinction (S^{OE}) and an underestimated photon absorption extinction (A^{UE}).

Step 2: Use the underestimated photon absorption extinction from Step 1 to correct the sample IFE in the PRS2 spectrum to obtain an underestimated light scattering extinction (S^{UE}) and a new overestimated light absorption extinction (A^{OE}).

Step 3: Calculate the mean-averaged maximum estimation errors in the light scattering extinction according Eq. 4. If the Err is less than 0.01 or other error limit, one can simply take the average of the S^{UE} and S^{OE} as the sample scattering extinction. Otherwise, use the new overestimated light absorption extinction A^{OE} from Step 2 to obtain a new S^{OE} and A^{UE}. The step 2 and 3 iterates until *Err* is below 0.01 or another desired threshold value set by the user.

$$Err = \frac{S^{OE} - S^{UE}}{(S^{OE} + S^{UE})/2} \quad \text{Eq. 4}$$

This iteration PRS2 method has been used for decomposing the experimental UV-vis extinction spectra of *f*PSNP (Fig. 4(A)) into its absorption and scattering extinction spectra (Fig. 4(C) and 4(E)). The average *Err* in the experimental light scattering extinction in the entire wavelength region from 400 nm to 650 nm decreases from 8.4×10^{-4}, 8.6×10^{-7}, to 1.0×10^{-9} when PRS2 method is iterated for the first, second, and third time (Fig. S2 and S3, ESI). The rapid converging between the over- and under-estimated light scattering extinction highlights efficiency of this iteration PRS2 method.

The Err threshold value of 0.01 is recommended to ensure there is no significant error in the IFE correction due to the ineffective estimation of the sample photon absorption extinction. Assuming the total photon extinction of a fluorescent sample is 1. An Err of 0.01 means the maximum overestimated or underestimated error in the scattering extinction (S^{OE}-S or S-S^{UE}) is no more than 0.01. In this case, the maximum underestimated or overestimated error in absorption extinction (A-A^{UE} or A^{OE}-A) in less than 0.01. Such a small estimation uncertainty in the photon absorption extinction should have negligible impact of the effectiveness of the sample IFE correction.

Correcting sample IFE on SSF in fluorescent NPs (*f*PSNP).

Equipped with the iteration PRS2 method, one can perform sample IFE correction on the fluorescence and light scattering measurement in samples with unknown scattering and absorption activities, demonstrated by *f*PSNP. The as-acquired *f*PSNP SSF spectra has severely distorted due to the sample IFE (Fig. 4(B), 4(G), and 4(H)). Overcorrection occurs when the photon extinction is used for the correcting the sample IFE (Fig. 4(D), 4(G) and 4(H)). However, excellent linearity is observed for IFE-corrected *f*PSNP fluorescence signal as a function of its concentration when only the sample photon absorption extinction is used for the IFE-correction (Fig. 4(F), 4(G), and 4(H)). This demonstrates again the importance of quantitative decoupling of the sample photon scattering and absorption extinction contribution to its UV-vis extinction spectrum for the sample IFE correction in SSF measurements. The fact that use of light absorption extinction spectra obtained with iteration PRS2 method yields nearly perfect IFE correction also confirms the effectiveness of this technique for experimental decomposition of the sample UV-vis extinction spectrum into its absorption and scattering component spectra.

Conclusion

We demonstrated in this work that photon scattering and absorption differs drastically in inducing the sample IFE on fluorescence, RS2, and PRS2 measurements. The light absorption induces significant sample IFE (>5% signal attenuation) as long as the collective sample absorption extinction at the emission wavelength and detection wavelength is larger than 0.05 ($10^{-0.025}$). This is estimated by assuming the effective excitation and detection pathlengths are both approximately 0.5 as observed for the 1 cm ×1 cm cuvette used in this work. No significant sample IFE is observed even when the collective light scattering extinction is as large as 0.90. Treating light scattering extinction the same as absorption extinction induces substantial overcorrection of the sample IFE in SSF measurements. For samples that contains significant photon scattering (S>0.02, for example), one should decompose the material UV-vis extinction spectra into its absorption and scattering component spectra, and perform the sample IFE correction using only photon absorption extinction. The iteration PRS2 method presented in this work proves to be a powerful tool for such spectral decomposition. Since this methodology can be readily implemented by researchers with access to common UV-vis spectrophotometers and spectrofluorometers, the presented technique and insights should have broad impact on the chemical research that involves quantitative understanding of material photon absorption, scattering, and emission that can currently occur in many realistic samples.

Conflicts of interest

There are no conflicts to declare.

Acknowledgements

This work was supported by NSF funds (CHE 1151057) and (EPS-0903787) provided to D.Z.

Notes and references

1. L. Yang, C. Cui, L. Wang, J. Lei and J. Zhang, *ACS Appl. Mater. Interfaces*, 2016, **8**, 19084-19091.
2. J.-N. Tisserant, R. Brönnimann, R. Hany, S. Jenatsch, F. A. Nüesch, R. Mezzenga, G.-L. Bona and J. Heier, *ACS Nano*, 2014, **8**, 10057-10065.
3. D. Gong, X. Zhu, Y. Tian, S.-C. Han, M. Deng, A. Iqbal, W. Liu, W. Qin and H. Guo, *Anal. Chem.*, 2017, **89**, 1801-1807.
4. D. Lu, J. Lei, L. Wang and J. Zhang, *J. Am. Chem. Soc.*, 2012, **134**, 8746-8749.
5. S. Knoppe and T. Verbiest, *J. Am. Chem. Soc.*, 2017, **139**, 14853-14856.
6. A. L. Holsteen, S. Raza, P. Fan, P. G. Kik and M. L. Brongersma, *Science*, 2017, **358**, 1407-1410.
7. J. X. Xu, K. Siriwardana, Y. Zhou, S. Zou and D. Zhang, *Anal. Chem.*, 2018, **90**, 785-793.
8. N. Watanabe, X. Li and M. Shibayama, *Macromolecules*, 2017, **50**, 9726-9733.
9. A. Ohshima, A. Momotake, T. Arai and R. Nagahata, *J. Phys. Chem. A*, 2005, **109**, 9731-9736.
10. C. B. Nettles, Y. Zhou, S. Zou and D. Zhang, *Anal. Chem.*, 2016, **88**, 2891-2898.
11. K. Siriwardana, B. C. N. Vithanage, S. Zou and D. Zhang, *Anal. Chem.*, 2017, **89**, 6686-6694.
12. S. A. Athukorale, Y. Zhou, S. Zou and D. Zhang, *Anal. Chem.*, 2017, **89**, 12705-12712.
13. S. P. Boulos, T. A. Davis, J. A. Yang, S. E. Lohse, A. M. Alkilany, L. A. Holland and C. J. Murphy, *Langmuir*, 2013, **29**, 14984-14996.
14. W. Zhai, C. Wang, P. Yu, Y. Wang and L. Mao, *Anal. Chem.*, 2014, **86**, 12206-12213.
15. J. A. Yang, B. J. Johnson, S. Wu, W. S. Woods, J. M. George and C. J. Murphy, *Langmuir*, 2013, **29**, 4603-4615.
16. Q. Gu and J. E. Kenny, *Anal. Chem.*, 2009, **81**, 420-426.
17. T. Wang, L.-H. Zeng and D.-L. Li, *Appl. Spectrosc. Rev.*, 2017, **52**, 883-908.
18. A. Archut, G. C. Azzellini, V. Balzani, L. De Cola and F. Vögtle, *J. Am. Chem. Soc.*, 1998, **120**, 12187-12191.
19. P. J. Collings, E. J. Gibbs, T. E. Starr, O. Vafek, C. Yee, L. A. Pomerance and R. F. Pasternack, *J. Phys. Chem. B*, 1999, **103**, 8474-8481.
20. N. Micali, F. Mallamace, M. Castriciano, A. Romeo and L. Monsú Scolaro, *Anal. Chem.*, 2001, **73**, 4958-4963.
21. B. Bhattacharyya and A. Pandey, *J. Am. Chem. Soc*, 2016, **138**, 10207-10213.
22. S. Kim, A. R. Marshall, D. M. Kroupa, E. M. Miller, J. M. Luther, S. Jeong and M. C. Beard, *ACS Nano*, 2015, **9**, 8157-8164.
23. M. L. Böhm, T. C. Jellicoe, M. Tabachnyk, N. J. L. K. Davis, F. Wisnivesky-Rocca-Rivarola, C. Ducati, B. Ehrler, A. A. Bakulin and N. C. Greenham, *Nano Lett.*, 2015, **15**, 7987-7993.
24. S. G. Liu, D. Luo, N. Li, W. Zhang, J. L. Lei, N. B. Li and H. Q. Luo, *ACS Appl. Mater. Interfaces*, 2016, **8**, 21700-21709.
25. H. Han, V. Valle and M. M. Maye, *J. Phys. Chem. C*, 2012, **116**, 22996-23003.
26. I. N. Evdokimov, A. A. Fesan and A. P. Losev, *Energy & Fuels*, 2016, **30**, 4494-4503.
27. M. Zhang, X. Cao, H. Li, F. Guan, J. Guo, F. Shen, Y. Luo, C. Sun and L. Zhang, *Food Chem.*, 2012, **135**, 1894-1900.
28. Y. Liu, H. Zang, L. Wang, W. Fu, W. Yuan, J. Wu, X. Jin, J. Han, C. Wu, Y. Wang, H. L. Xin, H. Chen and H. Li, *Chem. Mater.*, 2016, **28**, 7537-7543.
29. W. Zhai, C. Wang, P. Yu, Y. Wang and L. Mao, *Anal. Chem.*, 2014, **86**, 12206-12213.
30. Q. Gu and J. E. Kenny, *Anal. Chem.*, 2008, **81**, 420-426.
31. D. Atrahimovich, J. Vaya, H. Tavori and S. Khatib, *Journal of agricultural and food chemistry*, 2012, **60**, 3679-3685.
32. C. B. Nettles, J. Hu and D. Zhang, *Anal. Chem.*, 2015, **87**, 4917-4924.
33. M. Tarai and A. K. Mishra, *Anal Chim Acta*, 2016, **940**, 113-119.
34. J. C. Cancilla, P. Díaz-Rodríguez, J. G. Izquierdo, L. Bañares and J. S. Torrecilla, *Sensors and Actuators B: Chemical*, 2014, **198**, 173-179.
35. J. E. Cohen, P. Comon and X. Luciani, *Chemometrics and Intelligent Laboratory Systems*, 2016, **150**, 29-40.
36. A. I. Sulatskaya, A. V. Lavysh, A. A. Maskevich, I. M. Kuznetsova and K. K. Turoverov, *Sci Rep*, 2017, **7**, 2146.
37. Y. Shutova, A. Baker, J. Bridgeman and R. K. Henderson, *Environmental Science: Water Research & Technology*, 2016, **2**, 749-760.
38. B. Wu, M. Yang, R. Yin and S. Zhang, *Journal of Hazardous Materials*, 2017, **335**, 100-107.
39. A. Gobrecht, R. Bendoula, J. M. Roger and V. Bellon-Maurel, *Anal Chim Acta*, 2015, **853**, 486-494.
40. Z. Pan, J. Peng, Y. Chen, X. Zang, H. Peng, L. Bu, H. Xiao, Y. He, F. Chen and Y. Chen, *Microchem. J.*, 2018, **136**, 71-79.
41. Y. Liu, H. Wang, S. Li, H. Gong, C. Chen, X. Chen and C. Cai, *Sens. Actuators B Chem.*, 2018, **258**, 402-407.
42. Y. X. Wang, L. Li, Z. S. Xu, Q. Pan and G. W. Song, *J. Dispers. Sci. Technol.*, 2011, **32**, 114-119.
43. K. Siriwardana, C. B. Nettles, B. C. N. Vithanage, Y. Zhou, S. Zou and D. Zhang, *Anal. Chem.*, 2016, **88**, 9199-9206.
44. D. Zhang and C. B. Nettles, *J. Phys. Chem. C*, 2015, **119**, 7941-7948.
45. R. A. Alberty and G. G. Hammes, *J. of Phys. Chem.*, 1958, **62**, 154-159.
46. J. Janin, *Proteins: Structure, Function, and Bioinformatics*, 1998, **28**, 153-161.

Table of Content Entry